Pleomorphism and Iridescence in *Tenacibaculum geojense*

Elena K. Perry
Microbial Diversity Course 2017
Marine Biological Laboratory

Abstract

Marine bacteria in the genus *Tenacibaculum* display diverse cell types, ranging from short rods to long filaments to coccoidal forms, and many strains have also been reported to be iridescent. However, the conditions that favor different cell types in these bacteria are largely unknown, and the morphological or physiological features that contribute to iridescence are likewise incompletely resolved. Here, we attempted to shed light on these questions by using as our model organism *Tenacibaculum geojense* str. 17EP2, which was isolated from the seawater at Trunk River Beach. We uncovered a differential distribution of cell types across visually distinct regions of colonies grown on a rich medium, with longer cells prevailing at the edges of young colonies compared to the center. By contrast, cells from colonies grown on a low nutrient medium tended to be uniformly short. Preliminary experiments with time-lapses of growth at the single cell level on high versus low nutrient media likewise suggest that low nutrient availability biases the growth and division of *T. geojense* towards shorter cells. Fortuitously, a spontaneous mutant with increased iridescence also arose from our cultures of *T. geojense*. While the cell length distributions of the iridescent mutant were broadly similar to those of the wildtype, scanning electron microscopy revealed stark differences in cellular organization between the two colony types, reinforcing previous suggestions that highly ordered structures within biofilms may contribute to bacterial iridescence.

Address:

Elena K. Perry (eperry@caltech.edu), Division of Biology and Biological Engineering, California Institute of Technology, 1200 E. California Blvd. MC 147-75, Pasadena, CA 91125.

Introduction

When one is used to looking at cultures of *Esherichia coli*, *Pseudomonas aeruginosa*, or other common model bacteria that form rod-shaped cells of approximately equal lengths, a clonal bacterial population that contains diverse cell morphologies offers an intriguing developmental and evolutionary puzzle. The marine bacteria belonging to the family *Flavobacteriaceae*, and in particular the genus *Tenacibaculum*, offer a prime example of such morphological diversity, as many of these species form both short rods and long filaments, as well as spherical forms in aged cultures (Bowman, 2006, p. 681). In other heterotrophic bacteria, filamentation has been suggested to occur in response to environmental stresses or predation (Justice *et al.*, 2008). Cellular elongation can also be related to motility. For example, in *Flexibacter spp*., cells must exceed a certain length before acquiring gliding motility (Costenbader and Burchard, 1978), and in *Proteus mirabilis*, swarmer cells are markedly elongated compared to vegetative cells (Matsuyama *et al.*, 2000). However, within *Tenacibaculum*, the functional significance of morphological heterogeneity and the conditions under which different cell types may prevail are almost entirely unknown.

Along with heterogeneity of cell types, iridescence has also been reported in several marine bacteria, including *Tenacibaculum* (Kee, 2016; Mickol, 2016). Previous studies have suggested that bacterial iridescence requires gliding motility (Kee, 2016; Kientz *et al.*, 2016), and iridescence has additionally been correlated in *Cellulophaga lytica* with an unusual hexagonal arrangement of cells within biofilms (Kientz *et al.*, 2016). Nevertheless, the genetic basis, mechanisms, and potential functions of bacterial iridescence have not been completely characterized, and it remains to be seen whether they are common to all iridescent bacteria.

Here, we attempted to characterize the conditions under which a particular strain of *Tenacibaculum geojense* favors different cell types, including comparisons of planktonic and surface-associated growth, as well as high versus low nutrient environments. We also took advantage of a spontaneous iridescent mutant to investigate possible morphological and structural features that contribute to iridescence. Our results indicate that nutrient availability strongly influences the morphological heterogeneity of *T. geojense* populations, and that highly ordered cell-cell arrangements may be a conserved feature of iridescent bacteria.

Materials and Methods

Isolation and culture conditions

The strain of *T. geojense* used in this study, hereafter named *T. geojense* str. 17EP2, was isolated from a seawater sample (30 ppt salinity) collected near the outflow of Trunk River (Woods Hole, MA). A 1 mL aliquot sample was concentrated 10x by centrifuging and resuspending in 100 µL of sterile seawater base (342.2 mM NaCl, 14.8 mM $MgCl_2$, 1.0 mM $CaCl_2$, 6.71 mM KCl). The concentrate was spread-plated on Sea Water Complete (SWC) agar (Table 1). After 24 hrs of incubation at 30°C followed by 24 hrs at room temperature, a flat yellow colony with irregular edges appeared, along with approximately 20 other colonies of diverse morphology. Cells were picked from the yellow colony and restreaked three times for purity on SWC agar; single colonies appeared after 36-48 hrs of incubation at 30°C.

After isolation of a pure culture, cell lysate was prepared by boiling a single colony in 25 µL of Alkaline PEG (ALP: 60 g PEG 200 in 0.93 mL 2 M KOH and 39 mL H_2O, final pH 13.3-13.5) for 15 min. The 16S rRNA gene was PCR-amplified from the lysate using the universal bacterial primers 8F and 1391R and submitted for Sanger sequencing. The top sequence hit from nucleotide BLAST was *Tenacibaculum geojense* str. YCS-6 (NR_117983.1, 98% identity).

Table 1. Recipes for media used in this study.

Ingredients	**1x SWC**	**0.1x SWC**
1x seawater base (see above)	1000 mL	1000 mL
Bacto tryptone	5 g	0.5 g
Yeast extract	1 g	1 g
Glycerol	3 mL	1 mL
1 M MOPS, pH 7.2	5 mL	5 mL
Agar (for plates)	15 g	15 g

Isolation of iridescent mutant

Besides plain 1x SWC agar, the wildtype (WT) strain of *T. geojense* was also grown on black agar (1x SWC agar with 1% filter-sterilized Sheaffer Skrip black ink) to highlight possible iridescence, as several other *Tenacibaculum* strains isolated in the course have been reported to

be iridescent. While the wildtype strain was only weakly iridescent on black agar (with no noticeable iridescence under normal room lighting on plain SWC agar), two colonies on one of the black agar plates developed strongly iridescent green patches after five days of incubation at 30°C. We hypothesized that these green patches represented spontaneous mutants, and attempted to isolate these mutants by restreaking for purity on SWC agar. One of the putative iridescent (IR) mutants was successfully propagated through three restreaks, consistently displaying blue-green iridescence on black agar within 24 hrs and iridescent green colony edges on plain 1x SWC agar after 3-5 days.

Characterization of cell types

5 uL of overnight culture grown in SWC medium with shaking at 30°C were spotted onto 1x SWC agar or 0.1x SWC agar (Table 1) and incubated at 30°C. For initial characterization of morphotypes, cells were picked with a 200 µL pipette tip from different regions of the colonies, smeared on a glass slide with 2 µL of seawater base, and observed with phase contrast microscopy. For subsequent quantification of cell length distributions, cells from different regions of the colonies were resuspended in 10-20 µL of seawater base, and 1 µL of resuspended cells (or liquid culture diluted to OD_{600} 0.1-0.6) was spotted onto an agarose pad (1% agarose in SWC) and observed under phase contrast on a Zeiss Axio Imager.A2 microscope. Images were captured with an Axiocam 503 color camera, using the ZEN software (Zeiss).

Quantification of cell length distributions

All samples for quantification were imaged at 100x magnification, except for cells from colony edges grown on 1x SWC, which were imaged at 40x due to the presence of extremely long filaments. Colonies were grown and analyzed in triplicate. At least five fields of view encompassing a total of >200 cells were analyzed per replicate for samples imaged at 100x, and at least three fields of view with the same minimum cell total were analyzed for samples imaged at 40x. The fields of view were chosen essentially at random, as long as they contained a reasonable number of cells without excessive debris or many tightly clustered or overlapping cells (which severely hinder downstream analyses). Images were segmented using a Python script available as a Jupyter notebook (image_segmenting.ipynb) at https://github.com/pereleal1/tenacibaculum. In brief, a Laplacian of Gaussian filter was applied

to the images and the output was thresholded to yield a binary image, after which objects too small to be bacteria were removed. Objects touching the edges of the field of view were also removed to avoid partially-captured cells.

Segmented images were saved as 8-bit TIFF files and imported into Fiji. The images were "skeletonized" to yield the backbones of the cells using the Skeletonize 2D/3D plugin, and the skeletons were analyzed with the Analyze Skeleton 2D/3D function (found under Analyze → Skeleton). The "largest shortest path" calculated by this function represented the length of each cell (minus a small fraction of the length that is inherently lost during skeletonization). Cell length distributions were compared using the Wilcox rank sum test in R, and the distributions were plotted using the R package ggplot2.

Growth time-lapses at the single-cell level

WT was grown to stationary phase overnight in 1x SWC with shaking at 30°C. The overnight culture was diluted 1:10 in seawater base and 1 µL was spotted in the well of a 50 mm glass-bottomed culture dish (MatTek Corporation). This drop was covered with a piece of agarose pad (1% agarose in 1x or 0.1x SWC) the height of two stacked microscopy slides. Besides keeping the lid of the plate on throughout the time-lapse experiments, a coverslip was placed on top of the pad to minimize evaporation and image drift. Time-lapses were acquired on a Nikon Eclipse Ti2 microscope with a wide-field camera, taking phase contrast images at 100x magnification every five minutes for four hours.

The time-lapse images taken for growth on 0.1x SWC were flatfield-corrected using a Gaussian blur method in Fiji and segmented with the deep learning-based algorithm DeepScope (https://github.com/zbarry/DeepScope) by Zach Barry (Garner lab at Harvard). Cell length quantification was attempted in Fiji on the segmented images as described above. However, in the later frames of the time-lapse with dense clusters of cells, the Skeletonize plugin switched to returning the outlines rather than the backbones of each cell, preventing a simple measurement of cell length by this method. Time constraints also prevented segmentation of the time-lapse of growth on 1x SWC, thereby restricting the comparative analysis to qualitative observations.

Spectral characterization of iridescence

Spectra of light reflected from WT and IR colonies were acquired using an SR-1900 spectroradiometer (Spectral Evolution Inc.). The samples were illuminated with an Osram 8V/20W halogen photo optic lamp (model 64255) at maximum intensity, with the incoming light angle manually adjusted to either 31° or 38° and the receiving fiber optic end pointing straight down approximately 1 cm above the agar surface (Fig. 7c). A white reflecting block provided by Spectral Evolution was used as the reference for 100% reflectance.

Scanning Electron Microscopy (SEM)

One colony of WT and two colonies of IR were grown for SEM by spotting 5 uL of overnight culture on 1x SWC agar and incubating at 30°C for 24 hrs, followed by another four days at room temperature. Once the IR colonies had developed iridescent edges, blocks of agar containing each colony were cut out with a scalpel and prepared for SEM according to the protocol described by Fischer *et al.* (2012) for colonies grown on agar plates. It was imperative to prevent liquid from directly contacting the colonies until they had been thoroughly fixed; otherwise layers of the colonies would flake off and disperse until only a few sections of the bottommost layers remained attached to the agar. Thus, rather than submerging the colonies in an aldehyde fixative, the agar blocks with the colonies were first placed in 35 mm petri dishes with 800 μL of 1% osmium tetroxide in water, with the liquid touching the sides of the agar block but not contacting the colonies directly. The petri dishes were covered and left for one hour to allow preliminary fixing of the colonies by the osmium tetroxide vapors. Next, the osmium tetroxide solution was exchanged for an equal volume of 3.5% glutaraldehyde in 0.1 M cacodylate (CAC) buffer, and the colonies were again left to incubate at room temperature for one hour, without directly contacting the liquid. Following glutaraldehyde fixation, the agar blocks were washed twice with 800 uL of 0.1 M CAC buffer with a 30 min incubation per wash. The agar blocks were treated with 1% osmium tetroxide in 0.1 M CAC buffer for another hour, followed by two more 30 min washes with MilliQ water. Finally, the colonies were dehydrated by gentle submersion in an ethanol gradient of 50%, 70%, 80%, 90%, 95%, and 100% ethanol, for 20 min per step. The final step with 100% ethanol was repeated, and the colonies were then dried with hexamethyldisilazane (HMDS). The ethanol was first exchanged with 2:1 ethanol:HMDS for 20 min, followed by 1:2 ethanol:HMDS for 20 min, and finally 100% HMDS for 20 min. The last

step (100% HMDS) was repeated with fresh solvent, and excess HMDS was pipetted off until the solvent barely covered the colonies. The colonies were then left to air dry in a fume hood overnight with the lids of the petri dishes cracked open. Once dry, the colonies were mounted on stubs, sputter coated with platinum to a depth of 10 nm, and observed on a Zeiss Supra 40VP scanning electron microscope.

Results and Discussion

Cell morphology

T. geojense str. 17EP2 displays a variety of cell morphotypes under different conditions. During log phase growth in 1x SWC liquid cultures, the cells are rod shaped, with lengths ranging from ~1.5 μm to 50 μm or more. Similarly, in young colonies (< 24 hrs after spotting from overnight cultures), the majority of cells are rods ranging in length from ~1.5 μm to well over 100 μm, the latter being highly flexible filaments (Fig. 1a). DAPI staining of filtered cells revealed that most of these filaments have a non-uniform distribution of DNA, with the appearance of regularly-spaced internal segments (Fig. 1c). In addition to rod-shaped cells, spindle-shaped cells that bulge in the middle occasionally appear in colonies (Fig. 1a). In older cultures (stationary phase in liquid, or colonies > 24 hrs old), a phase-dark spherical form that stains brightly with DAPI becomes increasingly abundant, along with cells in the intermediate stages of budding off these spherical forms either from one end or from the middle (Fig. 1b). While these spherical forms appear similar to immature microcysts, such as those formed by *Sporocytophaga myxococcoides* (Reichenbach, 2006, p. 551), they were never observed to mature into an optically refractile form like that reported for the microcysts of *S. myxococcoides*. In addition, unlike typical microcysts, the spherical forms did not exhibit heat resistance upon a 10 min exposure to 58°C; no viable CFUs were recovered after this treatment. As the spherical forms have not been purified separately from the rod-shaped cells, their exact nature and function remain an open question.

Colony morphology

Wildtype (WT) colonies spotted on 1x SWC agar typically developed a thin, translucent outer ring surrounding a denser yellow middle region within 24 hrs of incubation at 30°C (Fig.

2a); however, for consistent results it was important that the agar plates be poured at least two days ahead of time, as the higher moisture content of newer plates sometimes caused irregular spreading and uneven development of colonies. Between 24-72 hrs, concentric yellow rings developed interior to the outermost translucent ring, separated from the dense orange-yellow central region of the colony by a ring of irregular spiky formations (Fig. 2b). The colonies did not appear iridescent under normal lighting, although a faint rainbow-like iridescence could be seen in the translucent edges under a dissecting microscope with bright illumination from an oblique overhead angle.

WT colonies spotted on 0.1x SWC remained thin and translucent throughout the first 24 hours of growth, with a slightly raised outer ring, and were a paler yellow than colonies grown on 1x SWC (Fig. 2c). Within 48 hrs, a thin outer ring appeared with the beginnings of irregular spreading projections. Within 72 hrs, the projections grew into spreading plumes that were iridescent green when illuminated from an oblique angle, while the center of the colony remained non-iridescent (Fig. 2d).

Colonies of the IR mutant appeared distinct from WT within 24 hrs of spotting onto 1x SWC agar: the central region was surrounded by two concentric raised rings, and the outermost translucent ring was narrower than in WT colonies at the same stage of development (Fig. 3a). After 3 days of incubation at 30°C, the outermost translucent ring developed a green iridescence (Fig. 3b). On 0.1x SWC agar, the IR mutant appeared mostly similar to WT, with thin, pale colonies that developed plume-like spreading edges within 72 hrs (Fig. 3c, d). Interestingly, however, far fewer spreading plumes appeared around the IR colonies compared to WT, and not all of the plumes were iridescent.

Distribution of cell lengths in different regions of WT and IR colonies

In WT colonies grown on 1x SWC agar, the cell length distributions differed significantly between the translucent edges and yellow centers at 24 hrs (Fig. 4a). Extremely long filaments were found predominantly at the edges, where they reached lengths of up to ~200 μm, whereas the maximum cell length observed in a colony center was ~80 μm, with cells from colony centers in two out of three replicates not exceeding 25 μm. Notably, while the maximum cell lengths at the edge versus the center of the colonies clearly differed, short cells were abundant in both regions. Nevertheless, the median cell length was significantly higher at the colony edges

compared to the centers ($p < 0.001$ for all replicates). Interestingly, the clear difference between the colony edges and centers was attenuated over time. By 72 hrs, median cell length no longer differed significantly between the two regions ($p > 0.05$ for all replicates), as the median cell length at the colony edges had decreased from an average median of 4.9 μm to an average median of 2.5 μm (Fig. 4b).

Compared to WT colonies grown on 1x SWC, cells from colonies grown on 0.1x SWC occupied a much narrower distribution of lengths and were strongly biased toward short cells, with a complete absence of filaments longer than 10 μm (Fig. 4c, d). The distributions on 0.1x SWC did not differ significantly between colony edges and centers, nor did the distributions change significantly between 24 hrs and 72 hrs.

Based on the observation that cells in the iridescent spreading edges of WT colonies grown on 0.1x SWC were much shorter than cells in the non-iridescent edges of WT colonies grown on 1x SWC, we wondered if a similar predominance of short cells might occur at the iridescent edges of IR mutant colonies. We therefore compared the cell length distributions of IR and WT colonies at the 72 hr time point, when the IR colonies have iridescent edges while the WT colonies remain non-iridescent. Cells at the edges of IR colonies tended to fall within a slightly narrower range of lengths than WT cells, with a higher median cell length ($p < 0.001$) but a shorter maximum observed length (90.8 μm in IR, 115.2 μm for WT) (Fig. 4e, f). However, it is possible that cells exceeding 90 μm in length were also present in IR colony edges and simply were not captured by our sample size. Overall, the differences in the distributions of cell lengths between IR and WT colonies were not nearly as stark as the difference between WT on 1x SWC versus 0.1x SWC.

Distribution of cell lengths in liquid culture under different nutritional conditions

Having observed a bias towards shorter cells in WT grown on 0.1x SWC agar versus 1x SWC agar, we asked whether a similar bias would be apparent in liquid cultures with the same media. Indeed, the maximum cell length observed across all replicates during log phase growth in 0.1x SWC was 22.4 μm, compared to 49.8 μm in 1x SWC (Fig. 5, b). The difference was even more stark during stationary phase, with a maximum observed cell length of 5.5 μm in 0.1x SWC compared to 64.9 μm in 1x SWC. The median cell length was also slightly but significantly lower during both log phase and stationary phase in 0.1x SWC compared to 1x

SWC ($p < 0.05$ for log phase; $p < 0.001$ for stationary phase). Interestingly, the median cell length in 1x SWC was also slightly but significantly higher in log phase than in stationary phase ($p < 0.001$ for all replicates).

Growth of WT at the single-cell level under different nutritional conditions

Time-constraints prevented proper segmentation and quantitative analysis of the growth time-lapses, due to the difficulty of computationally distinguishing closely clustered cells. Nevertheless, qualitative inspection of the time-lapses revealed potential differences in growth and division of *T. geojense* within the first few hours of exposure to low versus high nutrient media. On 0.1x SWC agarose, two cells that started out as relatively long (6.2 and 11.7 μm, compared to a median length of 1.7 μm in stationary phase liquid 1x SWC cultures) divided into shorter cells over time, and none of the shorter initial cells ($n = 139$) appeared to more than double in length before dividing, with some dividing even before doubling in length (Fig. 6a, b). On 1x SWC agarose, however, several cells that started out < 5 μm long more than doubled their length without dividing over the course of the four-hour experiment (Fig. 6c, d). Interestingly, on both types of media, the cell divisions appeared to be asymmetric, although the degree of asymmetry varied: some of the longer cells repeatedly pinched off daughter cells near one pole, whereas most of the shorter cells appeared to divide closer to their midpoint. In addition, on one occasion in the 0.1x SWC time-lapse, a single long cell simultaneously fragmented into three daughter cells.

Iridescence of WT versus the IR mutant

When streaked on black agar, the IR mutant developed a brilliant turquoise color with green iridescence within 48 hrs, whereas WT streaks developed a duller green color with relatively weak iridescence (Fig. 7a, b). Spectral measurements of reflected light from the two strains confirmed these observations quantitatively, with the IR mutant displaying a broader peak that was blue-shifted relative to WT (Fig. 7d). Specifically, the IR mutant peak covered the 489-504 nm range (i.e. blue-green), whereas the WT peaked at 522 nm (green). The WT peak was also much lower than the IR mutant peak, in accordance with its visibly weaker iridescence. The lower peak for WT could not be explained by slight variations in the exact height of the fiber

optic receiver above the bacterial surface, since raising the fiber optic receiver to approximately twice the original height still resulted in a higher peak for the IR mutant.

Cell organization within WT and IR colonies as revealed by SEM

While the distributions of cell lengths in WT and IR colonies at the 72 hr time point were largely similar to each other, SEM revealed stark differences in cell organization between the two strains. At the edges of the non-iridescent WT colony, the majority of cells appeared to be long filaments, similar to what was observed with phase contrast microscopy. The cells appeared to be largely disordered, with ropelike bundles of parallel filaments but also many filaments draped or woven in a variety of directions (Fig. 8c), reminiscent of the tangles of long filaments frequently seen in agarose pad mounts of resuspended cells from WT colony edges. There were also many large gaps between the bundles, although these may be an artefact of the sample dehydration and drying process. By contrast, at the edges of both IR colonies, long filaments were arranged into striking, tightly packed parallel arrays that covered the entire iridescent region (Fig. 8d, e). Notably, while both WT and IR colonies shrank considerably and wrinkled in places as a result of dehydration and drying, the glittery iridescence of the IR colonies was still visible under a dissecting microscope immediately before sputter coating, although the color had changed (Fig. 8a, b). SEM also revealed that the non-iridescent centers of the IR colonies consisted primarily of shorter cells and the spherical forms previously mentioned, and these cells did not appear to be organized in any structured manner (Fig. 8f).

Discussion

In this study, we have found that the growth and division patterns of *T. geojense* are tied to nutritional state, with low nutrient media strongly biasing the population towards shorter cells. The combined results of growth on different liquid media and growth time-lapses at the single cell level suggest that the prevalence of long filaments at colony edges compared to colony centers on 1x SWC agar at 24 hrs may be at least partially attributable to a general effect of nutrient availability, given that colony centers are presumably nutrient-depleted compared to colony edges. However, the fact that extremely long filaments (100-200 μm) appeared exclusively at WT colony edges, and not in liquid cultures or in IR colonies, suggests that other factors besides nutrient availability contribute to this morphological phenomenon. Some species

of *Flexibacter* (a genus into which the first described *Tenacibaculum* species was originally misclassified) undergo a similar alternation between extremely long, thread-like filaments at colony edges and short, fat rods at colony centers (Reichenbach, 2006, p. 549). In these bacteria, the long filaments have been shown to possess gliding motility, whereas the short rods are non-motile (Reichenbach, 2006, p. 549), which offers a ready explanation for the dominance of the long filaments at the spreading colony edges. Throughout all of the experiments performed in this study, however, no obvious difference in motility was seen between the long filaments and shorter rod forms of *T. geojense*. In fact, on the few occasions where individual cells were seen actively gliding on agarose pads, those cells were usually short rods. Moreover, colonies with extremely long filaments had smooth boundaries, rather than the flame-like projections typically associated with fast gliders, whereas the plume-like projections of colonies on low nutrient agar consisted entirely of relatively short cells. Thus, it seems possible that the relationship between cell length and motility is actually reversed to some degree in *T. geojense* compared to *Flexibacter spp*. Overall, the functional role of the long filaments remains unclear and deserves further study.

The asymmetric cell divisions seen in the single cell resolution growth time-lapses are intriguing, as a previous study has shown that asymmetric cell division in mycobacteria plays a key role in generating populations with heterogeneous cell lengths and elongation rates (Aldridge *et al.*, 2012). In the future, using a microfluidic device such as the one described in that study could facilitate a more rigorous analysis of elongation rates and asymmetry of division in *T. geojense*, as well as shed more light on the different physiological properties of long filaments versus short rods. It would also be interesting to pulse-label the cell walls of *T. geojense* cells with fluorescent amino acids in order to determine whether the growth is unipolar or bipolar; in mycobacteria, unipolar growth partially explains the heterogeneity of elongation rates, as daughter cells that do not inherit the old growth pole must take the time to synthesize a new growth pole (Aldridge *et al.*, 2012).

Regarding the spontaneous IR mutant, the highly organized sheets of parallel cells seen in iridescent regions of the colonies reinforce the notion that cell-cell organization plays a key role in bacterial iridescence. The reasons and mechanisms that underlie such organization, and whether iridescence is the goal or merely a by-product, remain unknown. Bacterial iridescence has previously been correlated with gliding motility (Kientz *et al.*, 2016), which is likely a

prerequisite for developing highly ordered arrays of cells. Iridescence also appeared to be correlated with motility in our WT strain, as only the spreading plumes at the edges of colonies on 0.1x SWC agar were iridescent. However, motility alone is not sufficient for iridescence, as many of the spreading plumes found around IR mutant colonies on 0.1x SWC agar were non-iridescent, contrary to what one might expect. Presumably, the bacteria must also produce one or more compounds that contribute to iridescence (see also this year's mini-project report by Chi Nguyen). Whole-genome sequencing of the WT and IR strains will likely shed additional light on the genetic and physical basis of iridescence in *T. geojense*.

Overall, this study has introduced *T. geojense* as an intriguing model organism for studying the development of heterogeneous cell populations within a single bacterial strain. In the future, it will be interesting to determine whether the mechanisms underlying heterogeneity of growth and division in other asymmetrically-dividing bacteria are conserved in the *Tenacibaculum* clade. The ground also appears to be wide open for discovering potentially novel factors that may influence the decision of a particular cell to continue growing or to divide—and if it chooses to divide, where along its axis and into how many daughter cells to divide at once. Finally, the presence of both iridescent and non-iridescent WT phenotypes under different conditions, as well as the spontaneous IR mutant, will also make this species an excellent model for studying the mechanisms and possible functions of bacterial iridescence.

Acknowledgments

I would like to thank Dianne Newman and Jared Leadbetter for supporting my attendance of this course and, along with all of the other instructors and the TAs, for the advice and encouragement they have offered on this project over the last few weeks. In particular, Kurt Hanselmann designed the setup for spectral measurements and patiently helped with troubleshooting; Sean Crosson and Aretha Fiebig reintroduced me to the wonders of Fiji/ImageJ; Matthew Tien helped with 16S rRNA gene sequencing; and Georgia Squyres provided invaluable advice and personal assistance with the time-lapse microscopy experiments and subsequent image processing and analysis. In addition, Kasia Hammar from the Central Microscopy Facility (CMF) at MBL facilitated the fixation of our samples for SEM by providing the necessary reagents, and David from the CMF sputter coated the samples and assisted with SEM imaging. Chi Nguyen and Nadia Herrera, the other two students who worked on

Tenacibaculum iridescence this year, were wonderful partners and sounding boards throughout this quest. Finally, I would like to thank the Center for Environmental Microbial Interactions (CEMI) at Caltech and the Holger & Friederun Jannasch Scholarship in Microbial Diversity for funding my attendance. Thanks to this course, I have discovered an interest in bacterial morphology that I never knew I had, and which I am sure I will carry with me in the future.

References

Aldridge, B.B., Fernandez-Suarez, M., Heller, D., Ambravaneswaran, V., Irimia, D., Toner, M., and Fortune, S. (2012) Asymmetry and aging of mycobacterial cells leads to variable growth and antibiotic susceptibility. *Science* **335**: 100–104.

Bowman, J. P. (2006) The marine clade of the family Flavobacteriaceae: the genera Aequorivita, Arenibacter, Cellulophaga, Croceibacter, Formosa, Gelidibacter, Gillisia, Maribacter, Mesonia, Muricauda, Polaribacter, Psychroflexus, Psychroserpens, Robiginitalea, Salegentibacter, Tenacibaculum, Ulvibacter, Vitellibacter and Zobellia. In *The Prokaryotes*, 3rd ed., Vol. 7. Dworkin, M., Falkow, S., Rosenberg, E., Schleifer, K-H., and Stackebrandt, E. (eds). New York: Springer.

Costenbader, C.J. and Burchard, R.P. (1978) Effect of cell length on gliding motility of Flexibacter. *J. Bacteriol.* **133**: 1517–1519.

Kee, L. (2016) Characterization of gliding and iridescent mutant in marine *Tenacibaculum discolor*. MBL Microbial Diversity course mini-project report.

Kientz, B., Luke, S., Vukusic, P., Péteri, R., Beaudry, C., Renault, T., et al. (2016) A unique self-organization of bacterial sub-communities creates iridescence in Cellulophaga lytica colony biofilms. *Sci. Rep.* **6**: 19906.

Matsuyama, T., Takagi, Y., Nakagawa, Y., Itoh, H., and Wakita, J. (2000) Dynamic aspects of the structured cell population in a swarming colony of Proteus mirabilis. *J. Bacteriol.* **182**: 385–393.

Mickol, R. (2016) Making a monster into a mutant: isolation and analysis of a *Tenacibaculum sp.*

Reichenbach, H. (2006) The order Cytophagales. In *The Prokaryotes*, 3rd ed., Vol. 7. Dworkin, M., Falkow, S., Rosenberg, E., Schleifer, K-H., and Stackebrandt, E. (eds). New York: Springer.

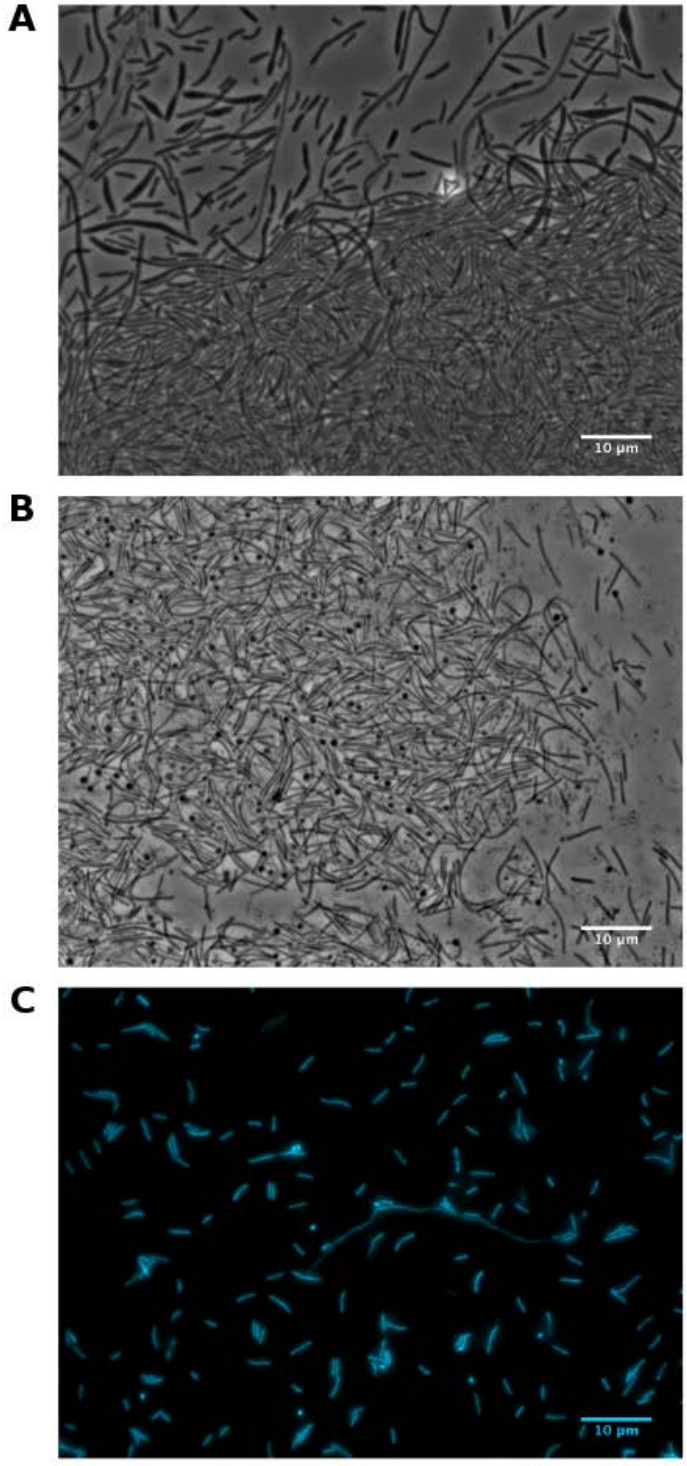

Figure 1. Images of cellular morphology of *T. geojense*. A) Cells from a 19-hr-old colony spotted on 1x SWC from an overnight culture, showing long filaments, short rods, and spindle-shaped cells. B) Cells from a 6-day-old colony, showing an abundance of spherical forms. C) DAPI stained cells from an overnight culture in 1x SWC.

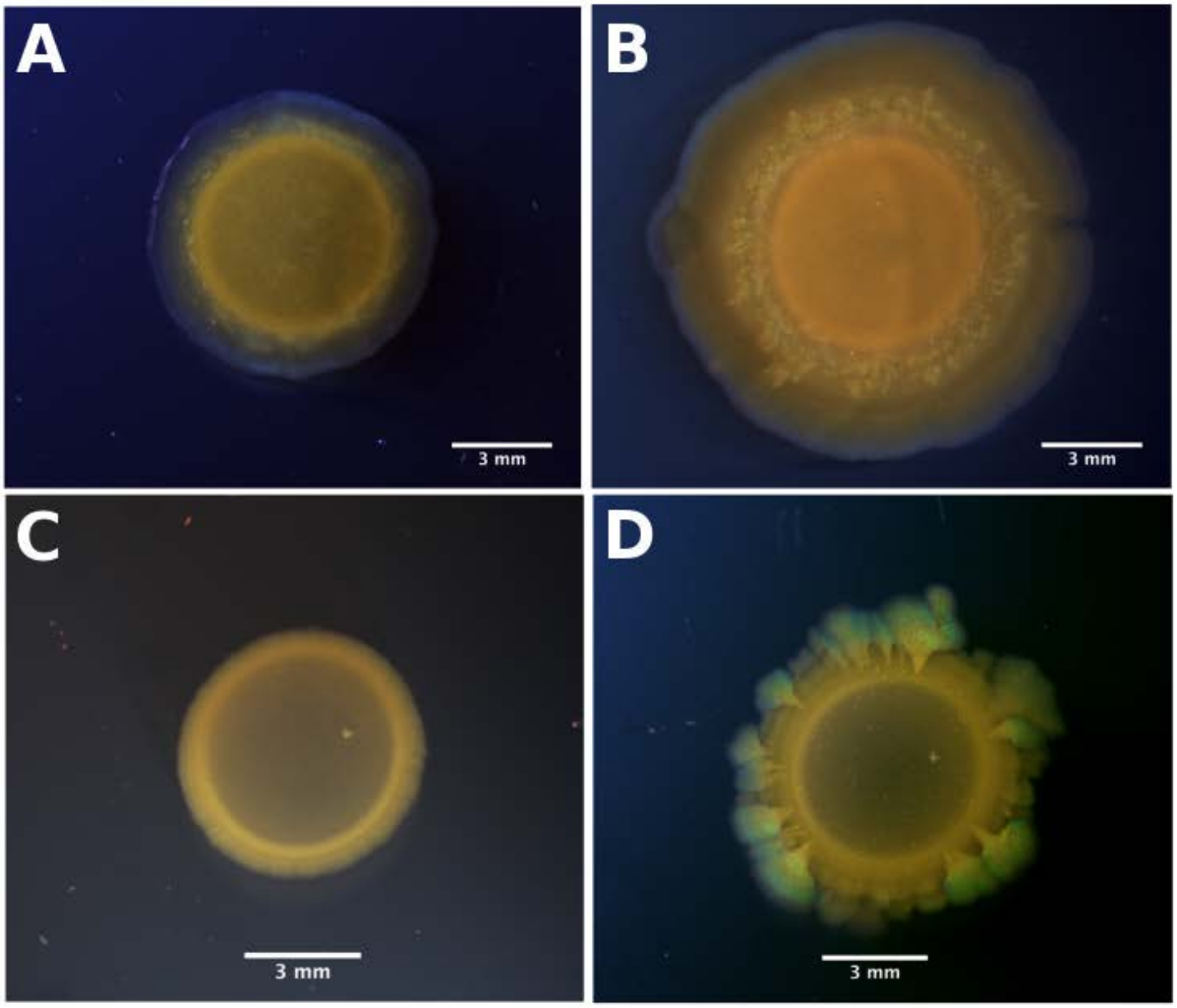

Figure 2. Morphology of WT colonies on different media. A) WT on 1x SWC agar after 24 hrs. B) WT on 1x SWC agar after 72 hrs. C) WT on 0.1x SWC agar after 24 hrs. D) WT on 0.1x SWC agar after 72 hrs.

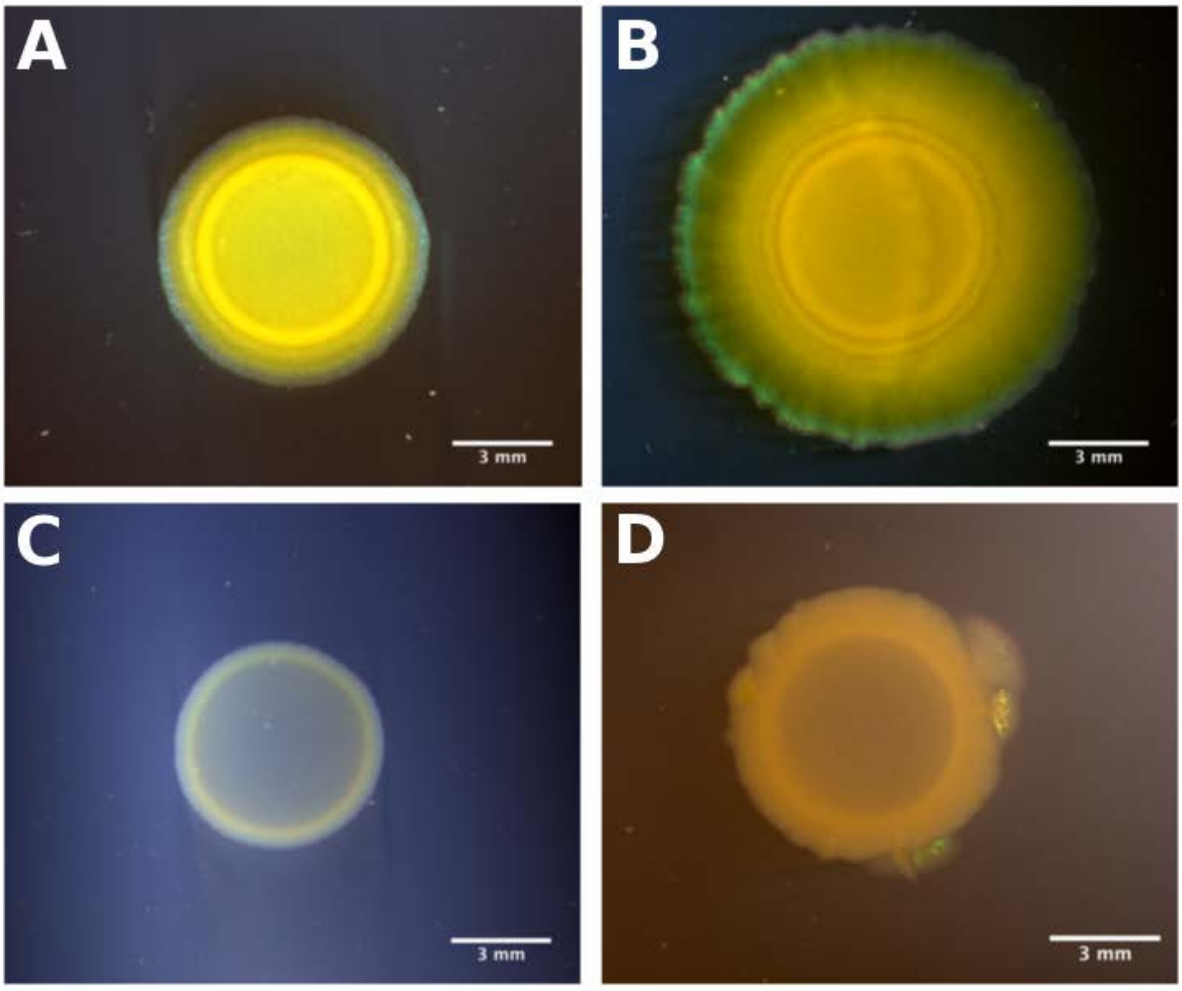

Figure 3. Morphology of IR colonies on different media. A) IR on 1x SWC agar after 24 hrs. B) IR on 1x SWC agar after 72 hrs. C) IR on 0.1x SWC agar after 24 hrs. D) IR on 0.1x SWC agar after 72 hrs.

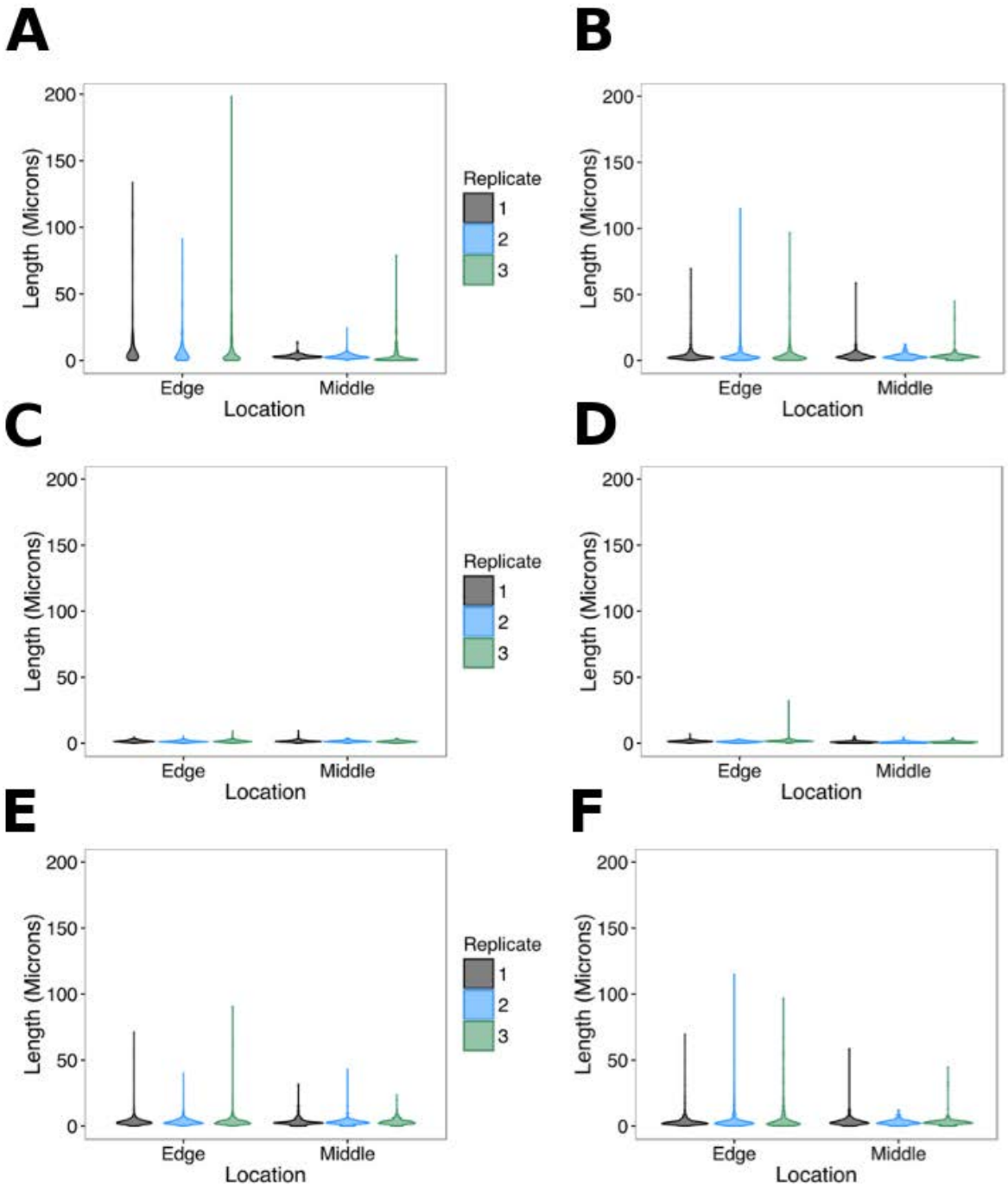

Figure 4. Distributions of cell length across time and space in WT and IR colonies on different agar media. A) WT on 1x SWC, 24 hrs. B) WT on 1x SWC, 72 hrs. C) WT on 0.1x SWC, 24 hrs. D) WT on 0.1x SWC, 72 hrs. E) IR on 1x SWC, 72 hrs. F) WT on 1x SWC, 72 hrs (repeat of B, for ease of comparison with E).

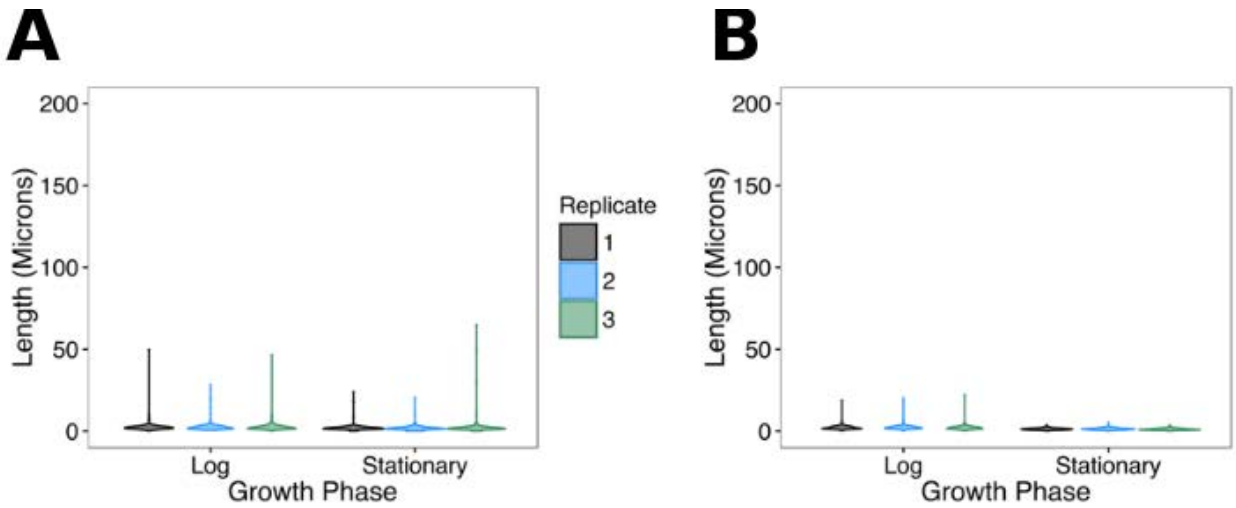

Figure 5. Distributions of cell length over time in different liquid media. A) WT in 1x SWC. Log phase samples were taken when the cultures had reached OD_{600} ~0.94 (6 hrs after inoculating 1:100 from an overnight culture), and stationary phase samples were taken at OD_{600} ~2.30 (32 hrs after inoculation). B) WT in 0.1x SWC. Log phase samples were taken when the cultures had reached OD_{600} ~0.29 (6 hrs after inoculating 1:100 from the same overnight cultures used for the 1x SWC inoculations), and stationary phase samples were taken at OD_{600} 0.42-0.54 (32 hrs after inoculation).

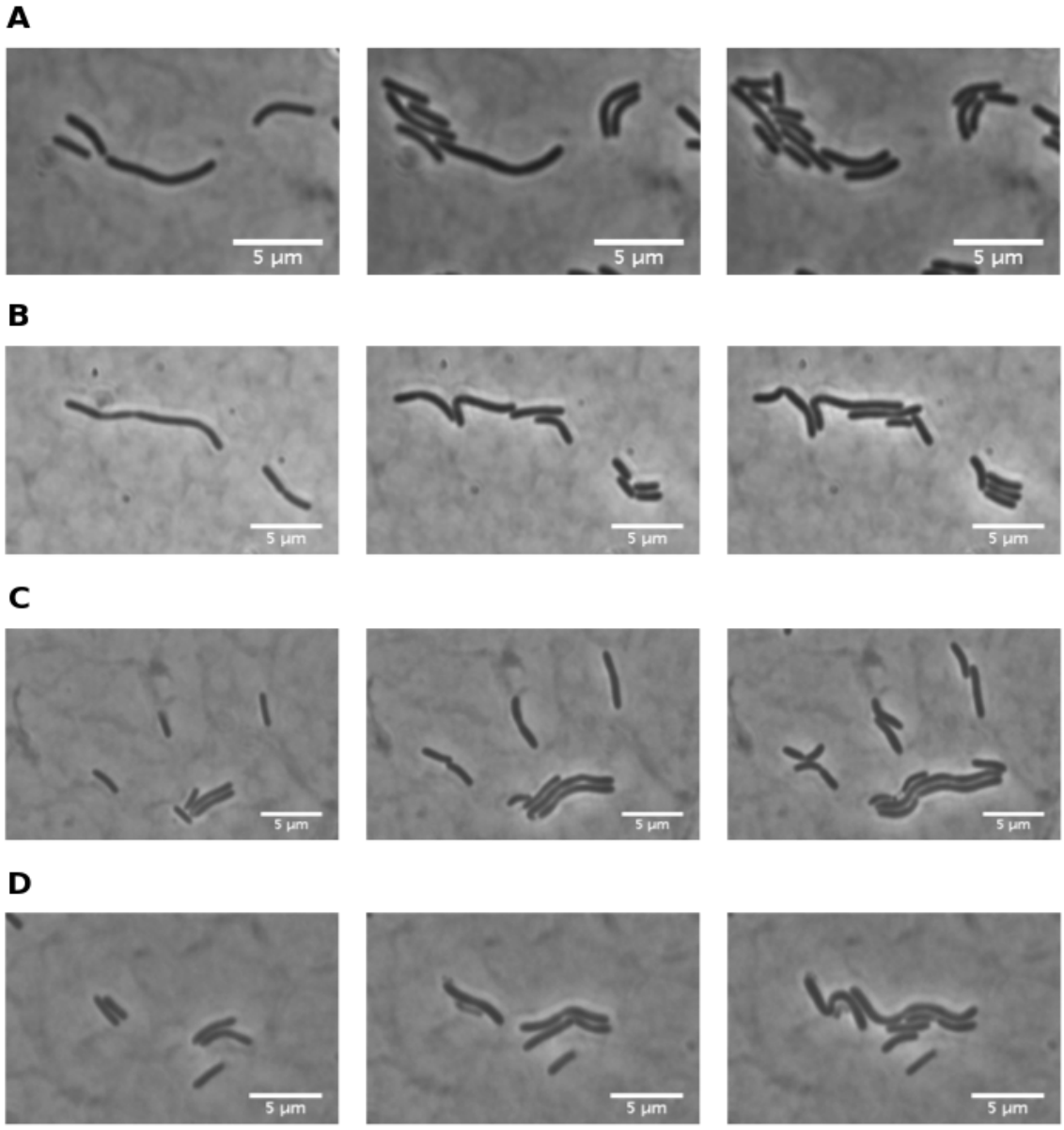

Figure 6. Stills taken from four-hour time lapses of WT growth on 1% agarose pads made with either 0.1x or 1x SWC. Pads were inoculated with 1 µL of 1:10 diluted overnight culture grown in 1x SWC. In order from left to right, stills are taken from time points 0 hr, 3 hr, and 4hr. A, B) Representative cells on 0.1x SWC that started out relatively long and divided into shorter daughter cells that in turn divided again before reaching as great a length as the original parent cell. C, D) Representative cells on 1x SWC that started out < 5 µm long and grew to more than twice their original length without dividing.

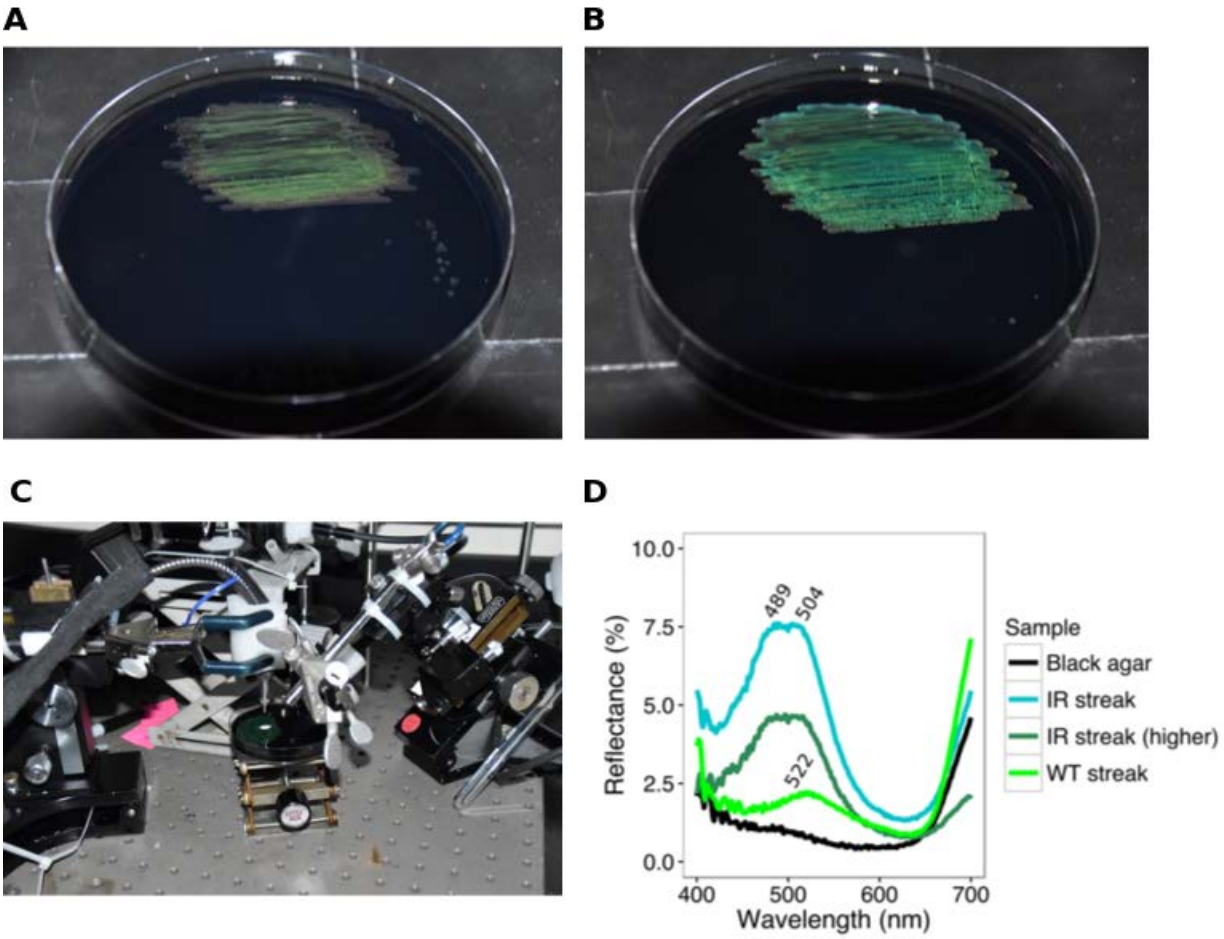

Figure 7. Spectral measurements of iridescence. A) WT appearance 48 hrs after streaking a loopful of overnight culture onto black agar. B) IR appearance 48 hrs after streaking a loopful of overnight culture onto black agar. C) Setup used for measuring spectra of reflected light, showing the fiber optic receiver clamped above the colony and the incoming light shining at an angle of 38°. D) Spectra of reflected light collected from the black agar (no bacteria), IR streak, IR streak from twice the usual height above the agar surface, and WT streak. Numbers above the spectra mark the wavelengths of peak reflectance. A white reflecting block provided by the manufacturer of the spectroradiometer was used as the reference for 100% reflectance.

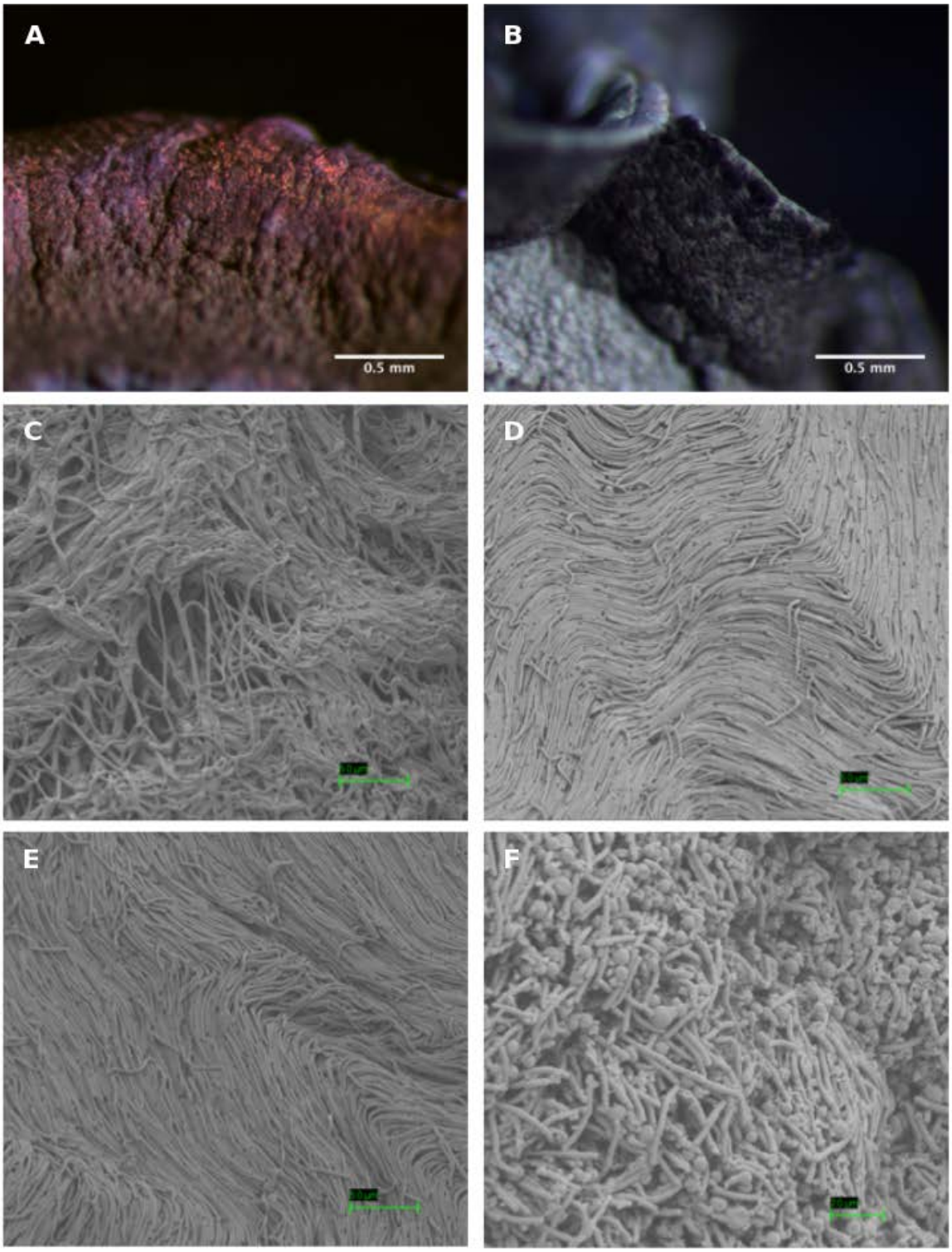

Figure 8. Scanning Electron Microscopy (SEM) images of WT and IR colonies. A) Iridescence still visible at the edge of an IR colony immediately prior to sputter coating. B) No iridescence apparent in the WT colony prior to sputter coating. C) Edge of WT colony. D) Edge of first IR colony. E) Edge of second IR colony. F) Center of first IR colony. Scale bar = 5 μm for C, D, and E; 2 μm for F.